

# Phosphomannopentaose sulfate (PI-88) suppresses angiogenesis by downregulating heparanase and vascular endothelial growth factor in an oxygen-induced retinal neovascularization animal model

Xian-Jun Liang,<sup>1,2</sup> Ling Yuan,<sup>1,3</sup> Jie Hu,<sup>1</sup> Hong-Hua Yu,<sup>1</sup> Tao Li,<sup>1</sup> Shao-Fen Lin,<sup>1</sup> Shi-Bo Tang<sup>1</sup>

(The first two authors contributed equally to this work)

<sup>1</sup>The State Key Laboratory of Ophthalmology Zhongshan Ophthalmic Center, Sun Yat-Sen University, Guangzhou, China; <sup>2</sup>Foshan Hospital of Traditional Chinese Medicine, Foshan, Guangdong, China; <sup>3</sup>The First Affiliated Hospital of Kunming Medical College, Kunming, Yuannan, China

**Purpose:** Vascular endothelial growth factor (VEGF) is the most potent angiogenic mitogen, and has been associated with angiogenesis. Heparanase is an endoglycosidase that specifically cleaves heparan sulfate side chains, which can induce VEGF expression. The aims of the present study were to evaluate the heparanase expression and its relationship with VEGF in the retina of oxygen-induced retinopathy (OIR) mice, and to investigate the effect of the heparanase inhibitor phosphomannopentaose sulfate (PI-88) in the OIR retinas.

**Methods:** Seventy-seven newborn C57BL/6 mice were involved in this study. On postnatal day 7 (P7), pups were exposed to a hyperoxia condition (75% oxygen) for 5 days, and on P12, the mice were returned to room air. Control mice were exposed to room air from birth until P17, with normally developing retinal vasculature. PI-88 was administered intraperitoneally to OIR mice at a dose of 35.7 mg/kg/day for 5 consecutive days. The expression level of heparanase and VEGF in the retinas was assayed using immunohistochemistry, Q-RT-PCR, and western blot.

**Results:** The expression levels of heparanase and VEGF were increased in the OIR retinas compared with the control mice. The Q-RT-PCR results showed that the mRNA expression levels of heparanase and *VEGF* in OIR retina were increased 1.71 fold ( $p<0.0001$ ) and 4.34 fold ( $p<0.0001$ ), respectively. The western blot results showed that the protein expression levels of heparanase and VEGF were increased 1.49 fold ( $p<0.0001$ ) and 1.72 fold ( $p<0.0001$ ), respectively, in the OIR retinas compared with the normal retinas. The immunohistochemistry analysis revealed that the heparanase and VEGF signals were intense in the retinal vascular endothelia of the OIR mice but faint in those of the normal controls. The increased protein and mRNA expression levels of heparanase and VEGF in the mouse retinas were significantly decreased by PI-88 administration ( $p<0.0001$ ).

**Conclusions:** Heparanase expression was upregulated and correlated with an increase in VEGF expression in the OIR mouse retinas, and might be involved in the progress of retinopathy of prematurity. Inhibition of heparanase expression by PI-88 could be used as a novel therapeutic method for retinopathy of prematurity.

Retinopathy of prematurity (ROP) is one of the leading causes of blindness in children worldwide, although considerable progress has recently been made in surgical strategies [1]. It is estimated that each year, 3,400 infants suffer from ROP-related visual impairments and 650 will become blind [2,3]. ROP is characterized by pathological ocular angiogenesis or retinal neovascularization (NV), mostly by exposure of low-birthweight infants to hyperbaric oxygen to maintain arterial oxygen tension in an appropriate range [4]. Nevertheless, the specific mechanism leading to ROP remains unknown and is difficult to study in human infants. Many molecules are involved in angiogenesis, of

which vascular endothelial growth factor (VEGF) is one of the best studied. VEGF stimulates the elongation of epithelial cells and subsequently can induce the formation of new vessels [5].

Heparanase is an endoglycosidase that degrades heparan sulfate (HS) in the extracellular matrix (ECM) and cell surface, and plays significant roles in cancer metastasis and angiogenesis [6]. Heparan sulfate proteoglycans (HSPGs) are macromolecules consisting of a protein core to which HS chains are linked [7]. HSPGs are present on the membranes of eukaryotic cells (i.e., syndecans and glypcans) or as molecules that are secreted into the ECM (i.e., perlecans). HS chains bind a large variety of molecules, such as ECM structural proteins, growth factors, chemokines, and enzymes, thereby participating in central biologic processes, including adhesion, proliferation, survival, and differentiation [7,8].

Correspondence to: ShiBo Tang, No.54 Xianlie Nan Road, Guangzhou 510060, China; Phone: +86 20 8733 0375 or 86 20 8733 0373; FAX: +86 20 8733 3271; email: tangsb@sysu.edu.cn

Therefore, cleavage of HS side chains is expected to not only alter the integrity of the extracellular matrix but also release HS-bound growth factors, chemokines, and cytokines. Meanwhile, HS fragments can modulate the activities of growth factors such as basic fibroblast growth factor and VEGF [9–11]. In addition, heparanase is actively involved in regulating *VEGF* gene expression via c-Src activation to promote angiogenesis [12].

Phosphomannopentaose sulfate (PI-88) is a synthetic polysulfated oligosaccharide that inhibits the activity of the extracellular matrix-degrading enzyme heparanase [13]. PI-88 is a 2-kDa heparan sulfate mimetic structurally distinct from heparin, which is a heterogeneous mixture of polysaccharide chains of varying lengths with molecular weights of 3 to 30 kDa. PI-88 was primarily developed as an antitumor agent and can potently inhibit tumor metastasis and angiogenesis [13–16]. Additionally, human and mammalian toxicology studies have demonstrated that PI-88 is well tolerated and has low anticoagulant activity [17]. PI-88 is currently in Phase II and III clinical trials to assess its therapeutic potential as an anticancer drug [14,18].

However, it is unknown whether heparanase is involved in ROP and contributes to angiogenesis, whether heparanase expression is closely related to VEGF expression in ROP, and whether heparanase could become a new therapeutic target for ROP. In this study, we investigated an oxygen-induced retinopathy (OIR) mouse model to try to answer these questions.

## METHODS

*Induction of oxygen-induced retinopathy and treatment:* The studies were approved by the animal care and use committee of Zhongshan Ophthalmic Center, Sun Yat-Sen University. We adopted the standard OIR model as described previously [19]. Seventy-seven specific pathogen free (SPF) newborn C57BL/6 mice were obtained from the Traditional Chinese Medicine Center for Animals of Guangzhou University. Food, water, light, temperature, and other conditions were the same for all animals. These mice were randomly divided into three groups: Group A, the control group (normal mice, n=25), was reared in the standard SPF level for the duration of the experiment. Group B was the OIR model group (OIR mice, n=26). Group C was OIR mice receiving PI-88 (Progen Industries Limited, Brisbane, Australia) (dissolved in sterile phosphate-buffered saline, PBS, pH 7.4) at a dose of 37.5 mg/kg/d intraperitoneally for 5 consecutive days (OIR mice +PI-88, n=26).

*Mouse model of oxygen-induced retinopathy and treatment:* The OIR mouse model was established as described previously [19]. Briefly, Group B and Group C mice were placed with their nursing mothers in the same covered plastic box with 75% oxygen from P7 (postnatal day 7) through P12. The oxygen was delivered at 75±2% and was checked at least

three times daily during the oxygen exposure period. The oxygen concentration was measured with an Oxygen Monitor (BioSpherix, Ltd., New York, NY). On P12, the animals were returned to room air for 5 days (P17). The Group C mice were injected with PI-88 at a dose of 35.7 mg/kg/day intraperitoneally for 5 consecutive days. Finally, all 77 mice were euthanized using a lethal intraperitoneal injection of chloral hydrate (360 mg/kg) at P17. The retinal tissues of all 77 mice were used for immunohistochemistry, Q-RT-PCR, and western blotting.

*Fluorescein isothiocyanate-dextran (FITC-Dextran) perfusion of the retinal blood vessels:* To study the retinal vascular pattern, systemic perfusion was performed using FITC-dextran (Sigma, St. Louis, MO) and polyphosphate-L-lysine (Sigma) in paraformaldehyde (PFA; Sigma). The animals were given a dose of 3 ml/kg chloral hydrate for anesthesia, and a median sternotomy was performed. The left ventricle of the heart was identified and perfused with 0.5 ml 4% PFA (50 mg/ml FITC-dextran and 10 mg/ml polyphosphate-L-lysine in 4% PFA) using a 1-ml tuberculin syringe with a 26-gauge needle for less than 30 s, until a yellowing of the liver was observed. The eyes of each mouse were then enucleated. Eyes were placed in 4% PFA for 30 min. Under a dissecting microscope (Axioplan2, ZEISS, Inc., Oberkochen, Germany), the retina was removed and flat-mounted by making radial cuts. Each retina was imaged with a fluorescence microscope (Axiovert100, ZEISS, Inc.).

*Immunohistochemistry staining for heparanase and vascular endothelial growth factor in oxygen-induced retinopathy retinas:* Immunohistochemistry was performed as previously described, with minor modifications [20]. Deparaffinized retinal sections were blocked in 3% hydrogen peroxide and 5% BSA (Sigma). Retinal sections were incubated overnight at 4 °C with polyclonal rabbit anti-rat heparanase-1 antibody (1:1,000; Abcam, Cambridge, MA) and VEGF antibody (1:1,000; Abcam). After being washed with PBS 3 times, sections were incubated with horseradish peroxidase-conjugated goat antirabbit immunoglobulin G (Invitrogen, Carlsbad, CA). Color was developed using a 3,3'-diaminobenzidine kit (Vector Laboratories, Burlingame, CA) for 5 min, followed by counterstaining with Mayer's hematoxylin. Immunostaining intensity was quantitatively analyzed using Image-Pro Plus software (version 5.1 for Windows; Media Cybernetics, Bethesda, MD) [21,22].

*Real-time polymerase chain reaction analysis for the expression of heparanase and vascular endothelial growth factor in oxygen-induced retinopathy retinas:* We extracted total RNA from retinas harvested from the different groups using TRIzol (Invitrogen). The concentration and purity of the RNA were determined with a spectrophotometer. The RNA was purified using Amplification Grade DNase I (AMPDI; Sigma), and reverse transcriptase (PrimeScript RT reagent Kit, DRR037A; TaKaRa, Shiga, Japan) was used to

synthesize cDNA. Q-RT-PCR assays were performed with SYBR Green Real-Time PCR Master Mix (SYBR Premix Ex Taq kit; TaKaRa), and gene expression was measured using SYBR green II (Qiagen, Hilden, Germany) with the ABI PRISM7000 real-time (Life Technologies Co., Ltd., Carlsbad, CA) PCR system. The PCR primers used to detect *VEGF*, heparanase, and *18S rRNA* were as follows: heparanase sense strand: 5'-CTC GAA GAA AGA CGG CTA AGA-3', and reverse strand: 5'-TGG TAG CAG TCC GTC CAT T-3'; *VEGF* sense strand: 5'-AAG GAG AGC AGA AGT CCC ATG A-3', and reverse strand: 5'-CAC AGG ACG GCT TGA AGA TGT-3'; *18S rRNA* sense strand: 5'-TTC CGA TAA CGA ACG AGA CTC T-3' and reverse strand: 5'-TGG CTG ACA CGC CAC TTG TC-3'.

*Western blot assay for the expression of heparanase and vascular endothelial growth factor in oxygen-induced retinopathy retinas:* Harvested retinas were homogenized in 150 µl lysis buffer containing 50 mM Tris-HCl (pH 6.8), 150 mM NaCl, 0.5% Triton X-100, and 10 µl protease inhibitor cocktail (Sigma-Aldrich, Inc., St. Louis, MO), and then centrifuged at 15,000×g at 4 °C for 30 min. Supernatants were collected and mixed with 5× sample loading buffer to prepare samples. Samples were electrophoresed on 12% sodium dodecyl sulfate gels and subsequently transferred to polyvinylidene difluoride membranes (Bio-Rad, Hercules, CA). Each membrane was blocked with 5% skim milk in Tris-buffered saline containing 0.5% Tween-20 at room temperature for 1 h. Next, the membranes were incubated with polyclonal rabbit antihuman heparanase-1 antibody (1:1,000) and polyclonal rat antihuman β-actin antibody (1:1,000; Abcam) at 4 °C overnight. The heparanase-1 antibody recognizes primarily the 50 kDa active form of the enzyme. The β-actin antibody recognizes primarily the 42 kDa active form of the enzyme. The membranes were then incubated with a secondary antibody at room temperature for 1 h. Finally, the blots were developed by a chemiluminescence kit (Cell Signaling Technology Inc., Danvers, MA). Semiquantitative analysis was performed by measuring the optical densities of the bands.

*Statistical analysis:* Data are presented as mean±standard deviation (SD). Statistical significance was analyzed with one-way ANOVA using GraphPad Prism 4.0 software system (GraphPad, San Diego, CA) and the statistical software program SPSS 16.0 for Windows (Chicago, IL). P values of <0.05 were considered significant in all cases.

## RESULTS

*Fluorescein isothiocyanate-Dextran systemic perfusion:* To determine whether the OIR mouse model was successfully established, FITC-dextran perfusion of the retinal blood vessels was observed under a fluorescent microscope in P17 OIR retinas. As shown in Figure 1A, fluorescence images showing retinal vessels were tortuous and expanded in volume. Capillary hemangioma was observed, and retinal

vascular morphology exhibited abnormal distribution at the junction of the perfused area and non-infused area. Significant expansion of large vessels, large avascular area, and extensive angiogenesis were observed. Thus, the OIR model was successfully established (Figure 1B).

*Immunohistochemistry staining analyses:* In the present study, the expression levels of heparanase and VEGF were increased in OIR retinal vascular endothelial cells (Figure 2B,E). Meanwhile, the expression levels of heparanase and VEGF were decreased in response to PI-88 treatment. Positive cells were stained red, and cytoplasmic staining was clearly observed in the retinal cells (Figure 2C,F). As shown in Figure 2B-F, the staining for heparanase and VEGF was intense in the endothelia of blood vessels in the OIR retinas but faint in those of normal retinas and OIR+PI-88 retinas.

Quantitative analysis of immunostaining fluorescence intensity showed that in vascular endothelial cells, the heparanase expression was increased in the OIR retinas compared with the normal retinas ( $p=0.003$ ), and decreased in the PI-88-treated OIR retinas compared with the OIR retinas ( $p=0.001$ ; Figure 2G). In vascular endothelial cells, the VEGF expression was significantly increased in the retinas of Group B compared with those of Group A ( $p<0.0001$ ) and decreased in Group C compared with Group B ( $p=0.001$ ; Figure 2H).

*Real-time polymerase chain reaction analysis:* We used real-time PCR to determine if the mRNA expression levels of heparanase and *VEGF* were changed in retinal vascular endothelial cells in OIR mice. The results indicated that the expression levels of heparanase and *VEGF* mRNAs increased in the OIR mice compared with Group A and Group C. In contrast, the expression of heparanase and *VEGF* was decreased by treatment with PI-88 (Group C). As shown in Figure 3A, the mRNA expression level of heparanase increased 1.71 fold in Group B compared with Group A ( $p<0.0001$ ), and the mRNA expression level of heparanase decreased 2.18 fold in Group C compared with Group B ( $p<0.0001$ ). There were significant differences in the heparanase expression level among the three groups ( $p<0.0001$ ). Compared with Group A, the mRNA expression level of *VEGF* increased 4.34 fold in Group B ( $p<0.0001$ ), Compared with Group B, the mRNA expression level of *VEGF* decreased 2.00 fold in Group C ( $p<0.0001$ ). There were significant differences in the *VEGF* expression level among the three groups ( $p<0.0001$ ; Figure 3B).

*Western blotting:* We used western blotting to investigate if the protein expression levels of heparanase and VEGF changed in the retinal vascular endothelial cells in the OIR mice. Western blot analysis for heparanase and VEGF demonstrated that the protein expression levels of heparanase and VEGF in the OIR mice increased (Figure 4A,B). Compared with Group A, the protein expression level of heparanase increased 1.49 fold in Group B ( $p=0.000$ ),

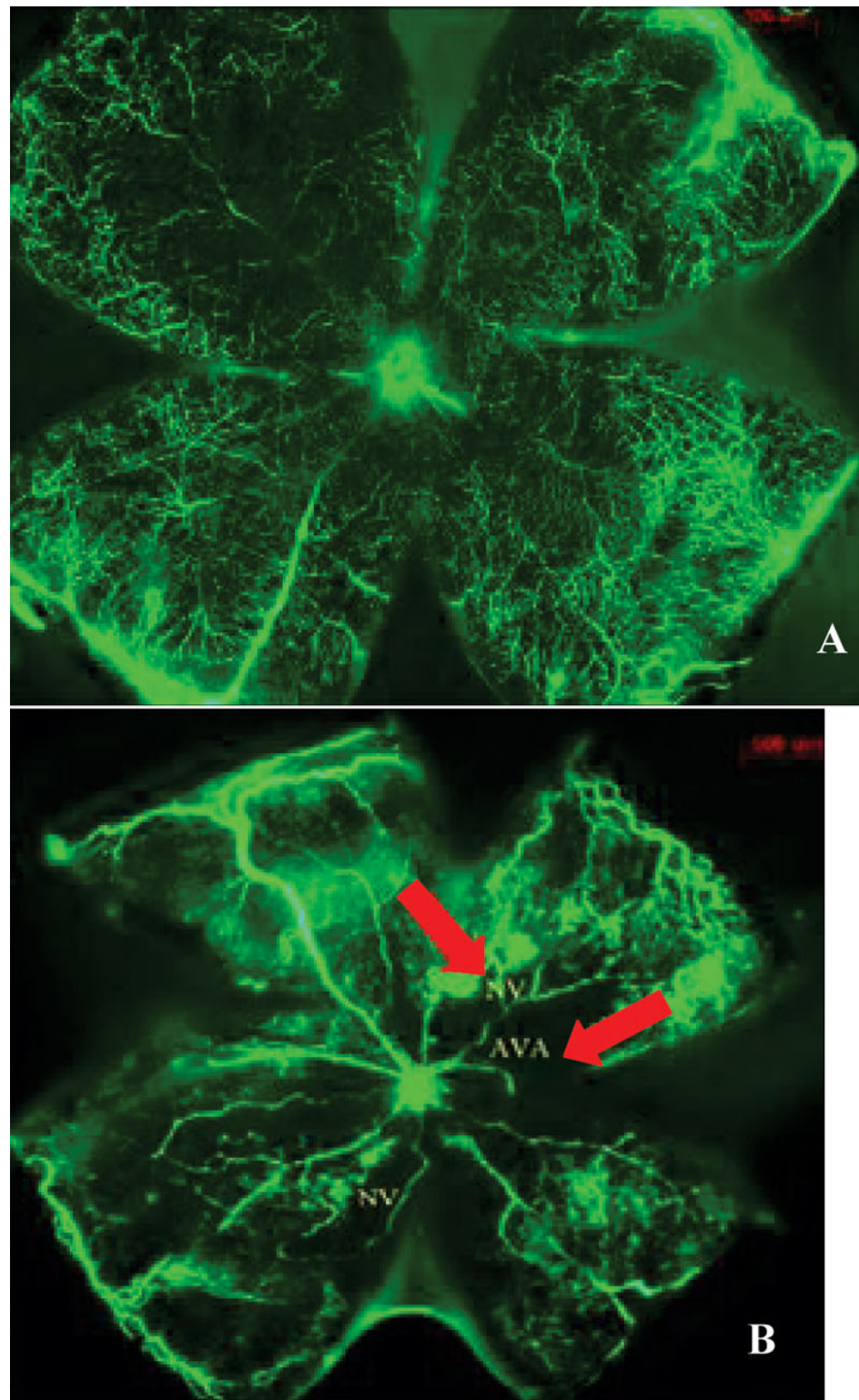


**Figure 1.** Fluorescein isothiocyanate-dextran (FITC) perfusion of the retinal blood vessels was observed under a fluorescent microscope in postnatal day 17 (P17) oxygen-induced retinopathy (OIR) retinas. **A:** Mice were perfused with FITC-labeled fluorescein sodium in normal oxygen pressure. **B:** Mice were perfused with FITC-labeled fluorescein sodium in hypoxia. Fluorescence images showing retinal vessels were tortuous and expanded in volume. Capillary hemangioma was observed, and retinal vascular morphology exhibited abnormal distribution at the junction of the perfused area and non-infused area. Significant expansion of large vessels, large avascular area, and extensive angiogenesis were observed. There are non-vascular area and neovascular tuffs in oxygen-induced retinopathy (OIR) mice (arrow).

Compared with Group B, the protein expression level of heparanase decreased 1.44 fold in Group C ( $p=0.000$ ). There were significant differences in the heparanase protein expression among the three groups ( $p<0.0001$ ; Figure 4C).

Additionally, compared with Group A, the protein expression level of VEGF increased 1.72 fold in Group B ( $p<0.0001$ ). Compared with Group B, the protein expression level of VEGF decreased 1.14 fold in Group C ( $p<0.0001$ ). There were

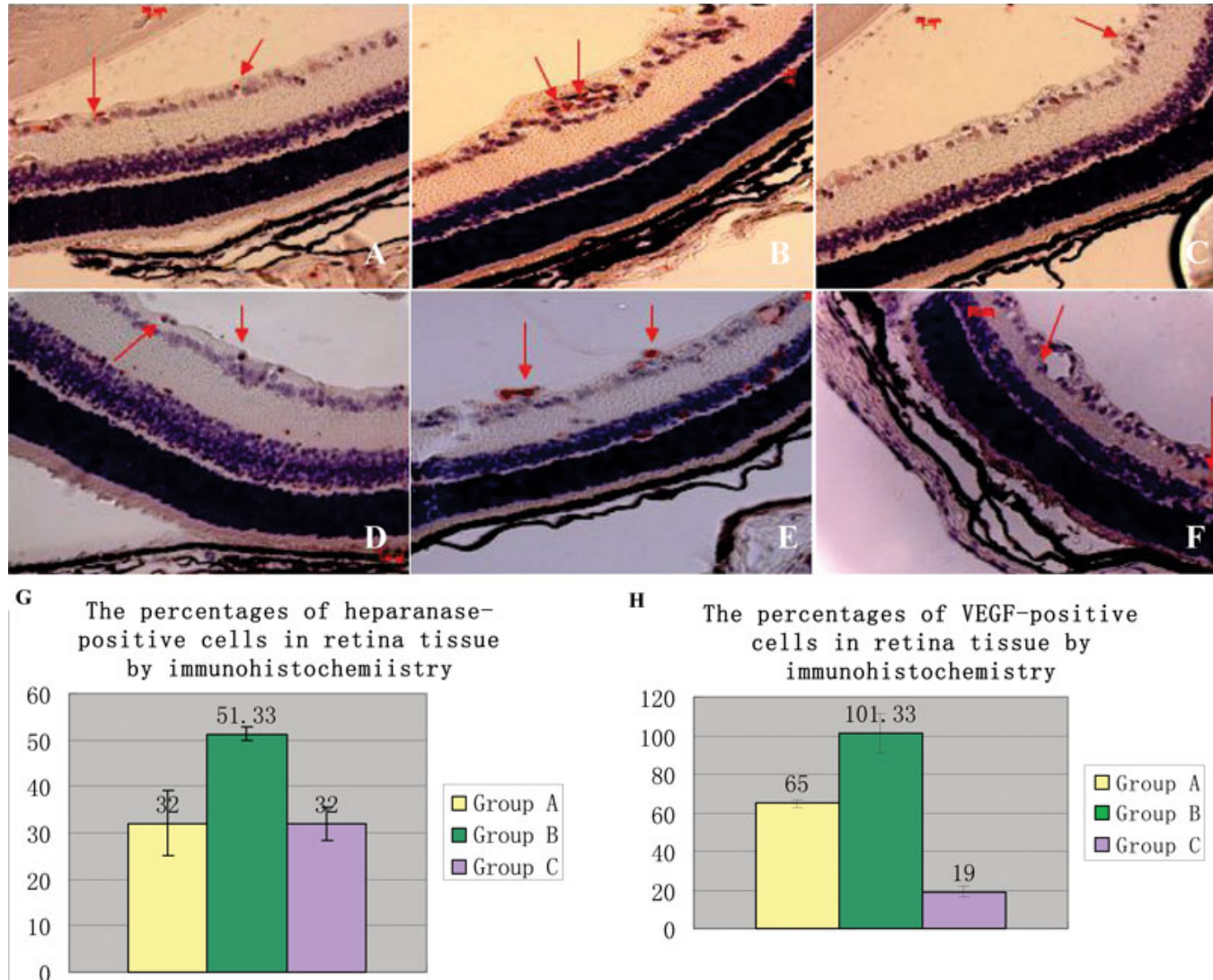


Figure 2. The effects of Immunohistochemistry staining for retina sections were assessed in this study. **A-C:** The retina sections stained for heparanase positive cells were shown. **A:** It shows a normal mouse retina section on postnatal day 17 (P17). **B:** It displays the retina section in oxygen-induced retinopathy (OIR) mice. **C:** It shows PI-88 treatment of an OIR mouse retina. In all of the sections, the red arrow points to heparanase positive cells. **D-F:** The retina sections stained for vascular endothelial growth factor (VEGF) positive cells were shown. **D:** It shows a normal mouse retina section on P17. **E:** It displays the retina section in OIR mice; **F:** It shows phosphomannopentaose sulfate (PI-88) treatment of an OIR mice retina. In all of the sections, the red arrow points to VEGF positive cells. **G:** The percentages of heparanase-positive cells in retina tissue by immunohistochemistry were as follows: The percentage of Group A was  $32.00\pm7.00$ ; the percentage of Group B was  $51.33\pm1.53$ ; the percentage Group C was  $32.00\pm3.61$ . **H:** The percentages of VEGF-positive cells in retina tissue by immunohistochemistry were as follows: The percentage of Group A was  $65.00\pm2.00$ . The percentage of Group B was  $101.33\pm10.11$ ; The percentage Group C was  $19.00\pm2.65$ . The differences among groups were significant ( $p<0.0001$ ).

significant differences in the VEGF protein expression among the three groups ( $p<0.0001$ ; Figure 4D).

## DISCUSSION

In the present study, we demonstrated that heparanase expression was significantly increased in the retinal vascular endothelia of OIR mice but there was faint staining in normal mice. Heparanase is an endoglycosidase that degrades heparan sulfate glycosaminoglycan, leading to the loss of

basement membrane integrity and the release of heparan sulfate-bound angiogenic and growth-promoting factors [23], which subsequently stimulate tumor blood vessel growth, cellular invasion, migration, adhesion, metastasis, differentiation, and proliferation [24–26]. Heparanase is overexpressed in a variety of tumors [27–32], corneal neovascularization [33], and the diabetic rat retina [34]. These findings suggest that heparanase expression is active in the vessel endothelium of newborn mouse retinas impaired by

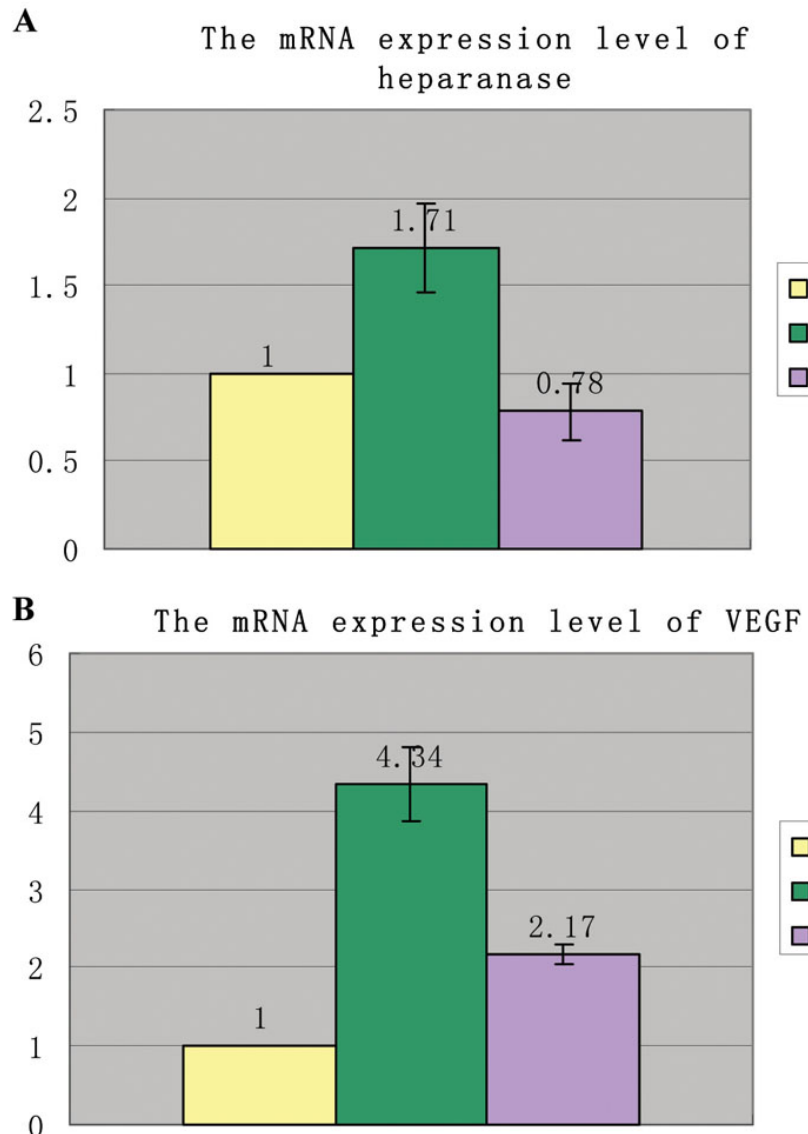


Figure 3. The effects of heparanase and vascular endothelial growth factor (VEGF) mRNA expression levels on oxygen-induced retinopathy (OIR) mice and normal mice were as follows. **A:** The mRNA expression level of heparanase increased 1.71 fold in Group B compared with Group A ( $p<0.0001$ ) but decreased 2.18 fold in PI-88-treated mice compared with the group B ( $p<0.0001$ ). There were significant differences in heparanase expression among the three groups ( $p<0.0001$ ). **B:** The mRNA expression level of vascular endothelial growth factor (VEGF) increased 4.34 fold in Group B compared with Group A ( $p<0.0001$ ) but decreased 2.00 fold in phosphomannopentaose sulfate (PI-88) treated mice compared with Group B ( $p<0.0001$ ). There were significant differences in VEGF expression among the three groups ( $p<0.0001$ ).

hyperoxia. Endothelial cells are an important cellular source of heparanase enzymatic activity [35–37].

Along with the high expression of heparanase, the expression of VEGF was also enhanced in OIR mice, as previously reported. Zetser et al. [12] reported that heparanase is actively involved in regulating *VEGF* gene expression. Heparanase expression is upregulated and is associated with increased VEGF expression in other retinopathy models, such as diabetic rats [34]. A novel mechanistic pathway driven by heparanase expression in myeloma cells can induce elevated levels of VEGF and shedding of syndecan-1 from matrix-anchored complexes that together activate integrin and VEGF receptors on adjacent endothelial cells, thereby stimulating tumor angiogenesis [38]. Cohen-Kaplan et al. [39] demonstrated that heparanase overexpression by epidermoid, breast, melanoma, and prostate carcinoma cells can induce a

three- to fivefold elevation in VEGF C expression in vitro, and heparanase gene silencing was associated with decreased VEGF C levels. Heparanase also seems to be actively involved in regulating *VEGF* gene expression via c-Src activation to promote angiogenesis [9]. Our results showed that the protein and mRNA expression levels of heparanase and VEGF were significantly increased in OIR retinas. These findings suggest that heparanase expression is upregulated by oxygen overexposure and has a close relationship with the VEGF level in OIR retinal vascular endothelial cells. Therefore, heparanase may be involved in the angiogenic responses of OIR mice via promoting VEGF expression.

Our study showed that the expression of heparanase and VEGF can be significantly decreased by PI-88 in OIR mice. Furthermore, PI-88 decreased the expression of heparanase in Group B and access to the expression of heparanase in Group

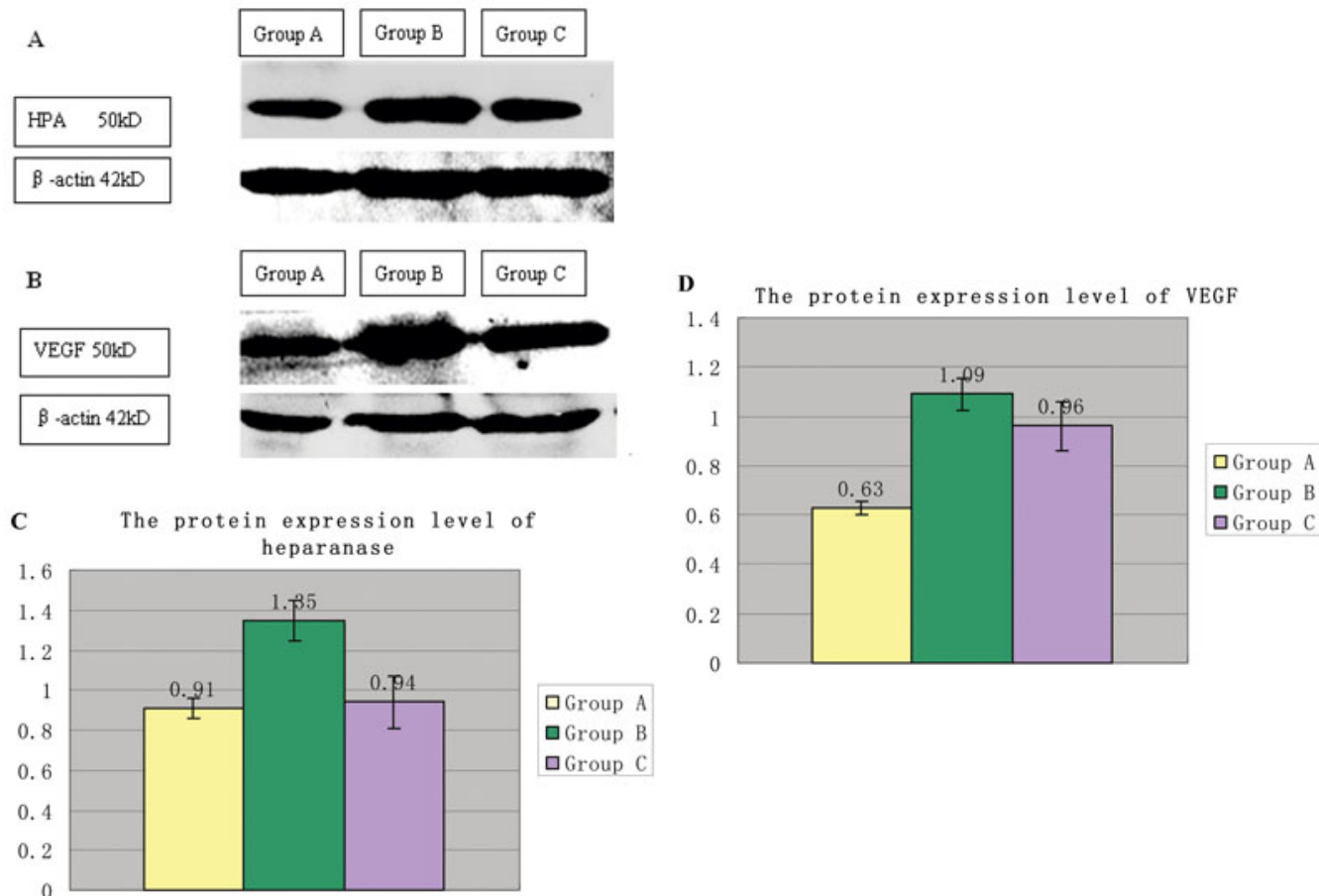


Figure 4. The effects of heparanase and vascular endothelial growth factor (VEGF) protein expression levels on three group mice were as follows. **A:** It shows the expression of heparanase in the three groups by western blot. The band that represents the 50 kDa activated enzyme was more intense in Group B than in Group A, and the level was decreased by phosphomannopentaose sulfate (PI-88) treatment. **B:** It shows the expression of VEGF in the three groups by western blot. The band that represents the 50 kDa activated enzyme was more intense in Group B than in Group A, and the level was decreased by PI-88 treatment. **C:** The protein expression level of Group B increased compared with Group A. There was a significant difference in the heparanase expression between the groups ( $p<0.0001$ ). **D:** The protein expression level in Group B increased compared with Group A. There was a significant difference in the VEGF expression between the groups ( $p<0.0001$ ).

A. Thus, PI-88 can decrease the expression of heparanase that it has increased due to oxygen induction. PI-88 is a mixture of highly sulfated oligosaccharides derived from the yeast *Pichia (Hansenula) holstii* NRRL Y-2488 and is a potent inhibitor of heparanase [13,40,41]. PI-88 shows antiangiogenic activity in vitro and in vivo, which is attributable to three known mechanisms: 1) inhibition of heparanase, an endoglycosidase that releases VEGF and active complexes of fibroblast growth factor by cleaving heparan sulfate proteoglycans in blood vessel basement membranes and the extracellular matrix; 2) direct inhibition of the binding of heparan sulfate to VEGF and fibroblast growth factor; and 3) stimulation of the release of tissue factor pathway inhibitor, an endogenous antiangiogenic protein [13,42,43]. In this study, treatment with PI-88 resulted in a decrease in the expression of VEGF and heparanase. Together, these results indicate the decreased VEGF

expression may be due to the inhibition of heparanase expression by PI-88 treatment.

In conclusion, our study, using the OIR mouse model, suggested that heparanase expression is upregulated in association with VEGF expression in OIR retinas, and inhibition of heparanase expression may be a novel therapeutic strategy for ROP. In a future study, we will focus on the mechanisms of hypoxia in upstream regulatory factor for heparanase expression, and shed light on the clinical treatment of ROP.

#### ACKNOWLEDGMENTS

This work was supported by grants from the Key Technology Introduction Projection of Guangdong Province/The International Cooperation Project of Guangdong Province (Grant No. 2008B050100038); the Fundamental Research Funds of State Key Lab of Ophthalmology, Sun Yat-Sen University (Grant No. 2010C04).

## REFERENCES

1. Chen J, Stahl A, Hellstrom A, Smith LE. Current update on retinopathy of prematurity: screening and treatment. *Curr Opin Pediatr* 2011; 23:173-8. [PMID: 21150442]
2. Gibson DL, Sheps SB, Uh SH, Schechter MT, McCormick AQ. Retinopathy of prematurity-induced blindness: birth weight-specific survival and the new epidemic. *Pediatrics* 1990; 86:405-12. [PMID: 2388790]
3. Penn JS, Rajaratnam VS, Collier RJ, Clark AF. The effect of an angiostatic steroid on neovascularization in a rat model of retinopathy of prematurity. *Invest Ophthalmol Vis Sci* 2001; 42:283-90. [PMID: 11133880]
4. Reynolds JD. ROP: A cautionary tale: what we know and what we think we know. *Am Orthopt J* 2010; 60:9-16. [PMID: 21061878]
5. Rajappa M, Saxena P, Kaur J. Ocular angiogenesis: mechanisms and recent advances in therapy. *Adv Clin Chem* 2010; 50:103-21. [PMID: 20521443]
6. Fuster MM, Wang L. Endothelial heparan sulfate in angiogenesis. *Prog Mol Biol Transl Sci*. 2010; 93:179-212. [PMID: 20807646]
7. Sasisekharan R, Shrimer Z, Venkataraman G, Narayanasami U. Roles of heparan-sulphate glycosaminoglycans in cancer. *Nat Rev Cancer* 2002; 2:521-8. [PMID: 12094238]
8. Bernfield M, Götte M, Park PW, Reizes O, Fitzgerald ML, Lincecum J, Zako M. Functions of cell surface heparan sulfate proteoglycans. *Annu Rev Biochem* 1999; 68:729-77. [PMID: 10872465]
9. Bame KJ. Heparanases: endoglycosidases that degrade heparan sulfate proteoglycans. *Glycobiology* 2001; 11:91R-8R. [PMID: 11445547]
10. Ilan N, Elkin M, Vlodavsky I. Regulation, function and clinical significance of heparanase in cancer metastasis and angiogenesis. *Int J Biochem Cell Biol* 2006; 38:2018-39. [PMID: 16901744]
11. Nasser NJ. Heparanase involvement in physiology and disease. *Cell Mol Life Sci* 2008; 65:1706-15. [PMID: 18425416]
12. Zetser A, Bashenko Y, Edovitsky E, Levy-Adam F, Vlodavsky I, Ilan N. Heparanase induces vascular endothelial growth factor expression: correlation with p38 phosphorylation levels and Src activation. *Cancer Res* 2006; 66:1455-63. [PMID: 16452201]
13. Parish CR, Freeman C, Brown KJ, Francis DJ, Cowden WB. Identification of sulfated oligosaccharide-based inhibitors of tumor growth and metastasis using novel in vitro assays for angiogenesis and heparanase activity. *Cancer Res* 1999; 59:3433-41. [PMID: 10416607]
14. Ferro V, Dredge K, Liu L, Hammond E, Bytheway I, Li C, Johnstone K, Karoli T, Davis K, Copeman E, Gautam A. PI-88 and novel heparan sulfate mimetics inhibit angiogenesis. *Semin Thromb Hemost* 2007; 33:557-68. [PMID: 17629854]
15. Khachigian LM, Parish CR. Phosphomannopentaose sulfate (PI-88): heparan sulfate mimetic with clinical potential in multiple vascular pathologies. *Cardiovasc Drug Rev* 2004; 22:1-6. [PMID: 14978514]
16. Kudchadkar R, Gonzalez R, Lewis KD. PI-88: a novel inhibitor of angiogenesis. *Expert Opin Investig Drugs* 2008; 17:1769-76. [PMID: 18922112]
17. Wall D, Douglas S, Ferro V, Cowden W, Parish C. Characterisation of the anticoagulant properties of a range of structurally diverse sulfated oligosaccharides. *Thromb Res* 2001; 103:325-35. [PMID: 11562342]
18. Lewis KD, Robinson WA, Millward MJ, Powell A, Price TJ, Thomson DB, Walpole ET, Haydon AM, Creese BR, Roberts KL, Zaleberg JR, Gonzalez R. A phase II study of the heparanase inhibitor PI-88 in patients with advanced melanoma. *Invest New Drugs* 2008; 26:89-94. [PMID: 17891338]
19. Smith LE, Wesolowski E, McLellan A, Kostyk SK, D'Amato R, Sullivan R, D'Amore PA. Oxygen-induced retinopathy in the mouse. *Invest Ophthalmol Vis Sci* 1994; 35:101-11. [PMID: 7507904]
20. Vlodavsky I, Friedmann Y, Elkin M, Aingorn H, Atzmon R, Ishai-Michaeli R, Bitan M, Pappo O, Peretz T, Michal I, Spector L, Pecker I. Mammalian heparanase: gene cloning, expression and function in tumor progression and metastasis. *Nat Med* 1999; 5:793-802. [PMID: 10395325]
21. Fumuso EA, Aguilar J, Giguere S, Rivulgo M, Wade J, Rogan D. Immune parameters in mares resistant and susceptible to persistent post-breeding endometritis: effects of immunomodulation. *Vet Immunol Immunopathol* 2007; 118:30-9. [PMID: 17559943]
22. Xavier LL, Viola GG, Ferraz AC, Da Cunha C, Deonizio JM, Netto CA, Achaval M. A simple and fast densitometric method for the analysis of tyrosine hydroxylase immunoreactivity in the substantia nigra pars compacta and in the ventral tegmental area. *Brain Res Brain Res Protoc* 2005; 16:58-64. [PMID: 16310404]
23. Yayon A, Klagsbrun M, Esko JD, Leder P, Ornitz DM. Cell surface, heparin-like molecules are required for binding of basic fibroblast growth factor to its high affinity receptor. *Cell* 1991; 64:841-8. [PMID: 1847668]
24. Edovitsky E, Elkin M, Zcharia E, Peretz T, Vlodavsky I. Heparanase gene silencing, tumor invasiveness, angiogenesis, and metastasis. *J Natl Cancer Inst* 2004; 96:1219-30. [PMID: 15316057]
25. Miao HQ, Liu H, Navarro E, Kussie P, Zhu Z. Development of heparanase inhibitors for anti-cancer therapy. *Curr Med Chem* 2006; 13:2101-11. [PMID: 16918340]
26. Xu X, Rao G, Quiros RM, Kim AW, Miao HQ, Brunn GJ, Platt JL, Gattuso P, Prinz RA. In vivo and in vitro degradation of heparan sulfate (HS) proteoglycans by HPR1 in pancreatic adenocarcinomas. Loss of cell surface HS suppresses fibroblast growth factor 2-mediated cell signaling and proliferation. *J Biol Chem* 2007; 282:2363-73. [PMID: 17121850]
27. El-Assal ON, Yamanoi A, Ono T, Kohno H, Nagasue N. The clinicopathological significance of heparanase and basic fibroblast growth factor expressions in hepatocellular carcinoma. *Clin Cancer Res* 2001; 7:1299-305. [PMID: 11350898]
28. Simizu S, Ishida K, Wierzbka MK, Sato TA, Osada H. Expression of heparanase in human tumor cell lines and human head and neck tumors. *Cancer Lett* 2003; 193:83-9. [PMID: 12691827]
29. Mikami S, Ohashi K, Katsume K, Nemoto T, Nakajima M, Okada Y. Coexpression of heparanase, basic fibroblast growth factor and vascular endothelial growth factor in

- human esophageal carcinomas. *Pathol Int* 2004; 54:556-63. [PMID: 15260846]
30. Cheng C, Lu X, Wang G, Zheng L, Shu X, Zhu S, Liu K, Wu K, Tong Q. Expression of SATB1 and heparanase in gastric cancer and its relationship to clinicopathologic features. *APMIS* 2010; 118:855-63. [PMID: 20955458]
  31. Shafat I, Ben-Arush MW, Issakov J, Meller I, Naroditsky I, Tortoreto M, Cassinelli G, Lanzi C, Pisano C, Ilan N, Vlodavsky I, Zunino F. Pre-clinical and clinical significance of heparanase in Ewing's sarcoma. *J Cell Mol Med* 2011; 15:1857-64. [PMID: 21029368]
  32. Yang Y, Ren Y, Ramani VC, Nan L, Suva LJ, Sanderson RD. Heparanase enhances local and systemic osteolysis in multiple myeloma by upregulating the expression and secretion of RANKL. *Cancer Res* 2010; 70:8329-38. [PMID: 20978204]
  33. Shi W, Liu J, Li M, Gao H, Wang T. Expression of MMP, HPSE, and FAP in stroma promoted corneal neovascularization induced by different etiological factors. *Curr Eye Res* 2010; 35:967-77. [PMID: 20958185]
  34. Ma P, Luo Y, Zhu X, Li T, Hu J, Tang S. Retinal heparanase expression in streptozotocin-induced diabetic rats. *Can J Ophthalmol* 2010; 45:46-51. [PMID: 20130710]
  35. Chen G, Wang D, Vikramadithyan R, Yagyu H, Saxena U, Pillarisetti S, Goldberg IJ. Inflammatory cytokines and fatty acids regulate endothelial cell heparanase expression. *Biochemistry* 2004; 43:4971-7. [PMID: 15109255]
  36. Edovitsky E, Lerner I, Zcharia E, Peretz T, Vlodavsky I, Elkin M. Role of endothelial heparanase in delayed-type hypersensitivity. *Blood* 2006; 107:3609-16. [PMID: 16384929]
  37. Fairbanks MB, Mildner AM, Leone JW, Cavey GS, Mathews WR, Drong RF, Slightom JL, Bienkowski MJ, Smith CW, Bannow CA, Heinrikson RL. Processing of the human heparanase precursor and evidence that the active enzyme is a heterodimer. *J Biol Chem* 1999; 274:29587-90. [PMID: 10514423]
  38. Purushothaman A, Uyama T, Kobayashi F, Yamada S, Sugahara K, Rapraeger AC, Sanderson RD. Heparanase-enhanced shedding of syndecan-1 by myeloma cells promotes endothelial invasion and angiogenesis. *Blood* 2010; 115:2449-57. [PMID: 20097882]
  39. Cohen-Kaplan V, Naroditsky I, Zetser A, Ilan N, Vlodavsky I, Doweck I. Heparanase induces VEGF C and facilitates tumor lymphangiogenesis. *Int J Cancer* 2008; 123:2566-73. [PMID: 18798279]
  40. Ferro V, Li C, Fewings K, Palermo MC, Linhardt RJ, Toida T. Determination of the composition of the oligosaccharide phosphate fraction of *Pichia (Hansenula) holstii* NRRL Y-2448 phosphomannan by capillary electrophoresis and HPLC. *Carbohydr Res* 2002; 337:139-46. [PMID: 11814445]
  41. Yu G, Gunay NS, Linhardt RJ, Toida T, Fareed J, Hoppensteadt DA, Shadid H, Ferro V, Li C, Fewings K, Palermo MC, Podger D. Preparation and anticoagulant activity of the phosphosulfomannan PI-88. *Eur J Med Chem* 2002; 37:783-91. [PMID: 12446036]
  42. Demir M, Iqbal O, Hoppensteadt DA, Piccolo P, Ahmad S, Schultz CL, Linhardt RJ, Fareed J. Anticoagulant and antiprotease profiles of a novel natural heparinomimetic mannopentaose phosphate sulfate (PI-88). *Clin Appl Thromb Hemost* 2001; 7:131-40. [PMID: 11292191]
  43. Cochran S, Li C, Fairweather JK, Kett WC, Coombe DR, Ferro V. Probing the interactions of phosphosulfomannans with angiogenic growth factors by surface plasmon resonance. *J Med Chem* 2003; 46:4601-8. [PMID: 14521421]

Articles are provided courtesy of Emory University and the Zhongshan Ophthalmic Center, Sun Yat-sen University, P.R. China. The print version of this article was created on 16 June 2012. This reflects all typographical corrections and errata to the article through that date. Details of any changes may be found in the online version of the article.